A Linearized Analog Microwave Photonic link with an Eliminated Even-order Distortions

Taimur N. Mirza, Shyqyri Haxha*, *Senior Member, IEEE and I. Dayoub, Senior Member IEEE.*

***Abstract*— An improved linearized Analog Microwave Photonic Link (AMPL) with significant multi-octave bandwidth performance is experimentally presented. The proposed AMPL configuration is based on a double dual-parallel Mach-Zehnder modulator and a differential balanced photodetector. Explicitly, a Gallium Arsenide (GaAs) based modulators are used as opposed to the commonly known Lithium Niobate ($LiNbO_3$) modulators, due to its robustness in the harsh environment. The system configuration is designed to process a carrier suppressed double-sideband signal through the link, and then at the receiver, a carrier suppressed double-sideband signal is combined with an unmodulated optical carrier, which is transmitted through a polarization maintained (PM) optical fiber. In our experiment, only PM based optical components are used for better system stability. The developed theoretical model of the proposed system illustrates the elimination of even-order distortions and a high suppression to the third-order intermodulation distortions (IMD3) at the balanced photodetector (BPD). Consequently, the fundamental Signal to Interference ratio (S/I) of 60dB was experimentally achieved. Furthermore, experimental results, simultaneously, demonstrate a significant increase of Second-order Spurious-free Dynamic Range (SFDR2) and Third-order Spurious-free Dynamic Range (SFDR3) by 19.5dB and 3.1dB, respectively, compared to the previously reported AMPL performances based on polarization multiplexing dual-parallel Mach Zehnder Modulator (PM-DPMZM). To the best of our knowledge, this is the highest dynamic range AMPL system performance deploying GaAs electro-optic (EO) modulator which has most significant capabilities in managing RF signals and exhibits excessive performance in harsh operating environment in terms of thermal stability, power-handling, radiation resistance and longevity for aerospace, defense, and satellite-to-ground downlink communication system applications.**

***Index Terms*—Electro-optic modulators, Harmonic Distortions, Intermodulation distortion, Microwave Photonics, Multi-Octave bandwidth.**

I. Introduction

Analog Photonic Link (APL) has a vast range of applications in defense as well as in commercial sectors, due to its intrinsic properties such as huge bandwidth, immunity to electromagnetic interference (EMI) and low losses [1-3]. The continuous growth in the usage of conventional communication networks has constrained the system capabilities, which now requires extensive improvements to the system performance [4-7]. One of the main contributors in the degradation of system performance is the transfer function of an external modulator. [8-9]. This performance is generally assessed by using performance indicators like spurious-free dynamic range (SFDR) and signal to interference ratio (S/I). These performance indicators show the level of distortion products in the RF spectrum. It is highly imperative to suppress the distortion products by using a linearization technique. Previously, various linearization techniques have been reported and some of them include the suppression of optical carrier (OC) by shifting the modulator's bias point, and by using the optical filters [10-13]. It is well known that optical carrier contains most of the optical power in the transmitted signal and the transmitted information is carried by the sidebands [10]. So, it is prudent to suppress the optical carrier through the transmission process. However, there are some other linearization techniques, which consider optimizing the modulator's transfer function to remove the distortion products. These techniques are often sub-octave in nature, and they limit the effectiveness in military and commercial applications [14-20]. Sub-octave systems generally bandwidth limited, and only certain distortions are required to be removed. Contrarily, multi-octave systems require the elimination of all the distortion products.

A lot of studies have been carried out in the past to suppress the IMD3 and IMD2, and to maximize the SFDR. However, the focus has been greatly on the suppression of the IMD3, as it lies close to the fundamental frequencies. This makes the system sub-octave, and the linearization techniques based on this system uses phase modulator [14], dual electrode Mach Zehnder modulator (DEMZM) [15-17], and dual-parallel Mach Zehnder modulators (DPMZM) [17-23]. An APL with phase modulator, polarizer, and an optical filter has been experimentally demonstrated [14]. But this technique is limited by optical filter's bandwidth and unable to suppress the IMD2 and IMD3 simultaneously. In [15], a two-path structure has been reported, where RF is modulated on one path, and an unmodulated optical carrier is transmitted through the second path. Both paths are coupled and detected by a single photodetector. However, a precise phase adjustment is required for the IMD3 cancellation. Similarly, a balanced photodetector has been used to eliminate the second-order harmonic distortions (SHD) [16]. Optical wave shaper has also been reported to linearize the APL [17], but it

Acknowledgment: This work was supported in part by the Leonardo MW Ltd trading as Leonardo Airborne & Space Systems Division, under the R11052 project collaboration.

Dr. Taimur N. Mirza and Dr. Shyqyri Haxha (contact author) is with the Department of Electronics Engineering, Royal Holloway University of London, Egham Hill, Egham, Surrey, TW20 0EX, United Kingdom (e-mail: Shyqyri.Haxha@rhul.ac.uk).

Prof. Iyad Dayoub is with the Institute of Electronic, Microelectronic & Nanotechnology (IEMN CNRS). Université de Valenciennes et du Hainaut-Cambrésis Le Mont-Houy, France.

makes the link highly dependent on the bandwidth of the wave shaper. Furthermore, in [18], two parallel MZMs has been used to reduce the noise figure and enhance the SFDR, but the model is limited to a precise polarization control. In [19, 20], a DPMZM structure with a complicated phase control of the RF input signal is demonstrated, where the Sub-MZMs are used to modulate the microwave signals to produce symmetrical single sidebands (SSB). However, it is very challenging to achieve the balance of the symmetrical SSBs.

The above-reported techniques are only based on a sub-octave system, and comparatively, little work has been reported on the simultaneous elimination of IMD2 and IMD3, which makes the system multi-octave [21]. A PM-DPMZM represents the two parallel DPMZM structures and by accurately adjusting the bias conditions, IMD3, IMD2, and SHD can be suppressed [22, 23]. The suppression of distortion products mainly depends on the DC bias voltage which is difficult to control manually. In [24], a multi-octave linearized system is proposed, which is also based on the PM-DPMZM and balanced photodetector (BPD). This research work [24] experimentally demonstrates the performance, and they report SFDR2 and SFDR3 of 95.5dB.Hz$^{1/2}$ and 123.9dB.Hz$^{2/3}$. However, the working of this system depends only on the precise control of DC bias shifting of the modulator, which is considered highly unstable. Another multi-octave system based on a phase modulator and a BPD is presented in [25]. The suppression of IMD2 and IMD3 is realized simultaneously by using the BPD and the phase modulation with optical sideband filtering. However, the bandwidth of the system becomes limited by the bandwidth of OBPF.

In this paper, a linearized APL is proposed and the linearity of the APL link is tested by using a two-tones. Two independent GaAs based DPMZMs are used in the proposed structure, which has many benefits over $LiNbO_3$ modulators, such as they are thermally stable and operate over a broad range of temperatures without causing any bias-point drift [26, 27]. These intrinsic properties of GaAs modulators make them highly suitable for harsh operating environment. In the proposed configuration, two electrical input ports of each DPMZM have a phase difference of 180º, which is generated by using a microwave phase shifter. Additionally, DPMZMs are biased to suppress the optical carrier, which essentially improve the system performance by reducing the effects of fiber nonlinearities [11]. It should also be noted that optical carrier is critical for the recovery of fundamental frequencies at the receiver. Therefore, an unmodulated optical carrier is transmitted through a PM fiber, which is then coupled with the carrier-suppressed modulated signal. This coupled signal is detected by a BPD and the even-order distortions are eliminated due to its differential function. The performance of our proposed system has been compared with the previously reported configurations based on a PM-DPMZM [22, 24]. We have experimentally demonstrated the SFDR performance of our proposed system, which is measured to be 115dB.Hz$^{1/2}$ and 127dB.Hz$^{2/3}$.

II. Mathematical Model Description of the AMPL Operation

The schematic diagram of the proposed linearized multi-octave system is illustrated in Fig. 1. The modulation section of the system comprises of two dual-parallel Mach Zehnder Modulators (DPMZM), which is named as double dual parallel Mach Zehnder Modulator (D-DPMZM). The transmitted light from the laser is equally (50:50) split; 50% is fed to the inputs of D-DPMZM, and the other 50% is transmitted to the receiver-end over an optical fiber, which is then coupled with a reference modulated signal before being detected by the BPD. E_c denotes the light beam, with its angular frequency of ω_c. Two input RF signals are combined and then equally split. Each DPMZM has two push-pull configured sub-MZMs that are fed with two-tone signals, and the input to both the sub-MZMs has a phase difference of 180°, as it is shown in Fig.1. A 180° phase shifter is used because both RF ports of the DPMZM are injected with the same signals, it would be logical to have that 180° out of phase so that the fundamental sidebands don't cancel out at the parent MZM (MZM_{13}, MZM_{23}) due to the destructive interference. RF_1 and RF_2 represent the two-tone RF signals, and their angular frequency is denoted as ω_1 and ω_2, respectively. The RF phase shift and the modulator's operating points contribute to suppressing the optical carrier. An external DC bias (V_{bias}) is used to control the operating points of each sub-MZM (MZM_{ij}; i=1, 2; j= 1, 2, 3) in order to achieve maximum suppression of an optical carrier and even-order distortions. The transfer function at the output of DPMZM1 and DPMZM2 can be expressed as;

$$E_{DPMZM_1}(t)=\frac{E_c}{2}e^{j\omega_c t}\left[\cos\left(\frac{\phi_{11}(t)}{2}\right)+e^{j\phi_{13}}\cos\left(\frac{\phi_{12}(t)}{2}\right)\right]. \quad (1)$$

$$E_{DPMZM_2}(t)=\frac{E_c}{2}e^{j\omega_c t}\left[\cos\left(\frac{\phi_{21}(t)}{2}\right)+e^{j\phi_{23}}\cos\left(\frac{\phi_{22}(t)}{2}\right)\right]. \quad (2)$$

The transfer function of a phase change $\phi_{ij}(t)$ in each MZM_{ij} can be further simplified by evaluating (1) and (2), which is caused by a modulating voltage of RF signal and a DC bias, can be represented as;

$$\left.\begin{aligned}\phi_{11}(t)&=\phi_{m1}(t)+\phi_{11}\\ \phi_{12}(t)&=\phi'_{m1}(t)+\phi_{12}\\ \phi_{21}(t)&=\phi_{m2}(t)+\phi_{21}\\ \phi_{22}(t)&=\phi'_{m2}(t)+\phi_{22}\end{aligned}\right\} \quad (3)$$

In (3), the phase difference caused by DC bias and the input RF signals are described by $\phi_{ij}=\pi V_{biasij}/V_{\pi i}$, and $\phi_{mi}(t)$ (i=1, 2; j= 1, 2, 3), respectively. Similarly, $\phi'_{mi}(t)$ represents the input RF signals with a 180° of phase shift, which is induced by an external RF phase shifter. The transfer function of the phase change caused by modulating voltages can be expressed as below;

$$\left.\begin{aligned}\phi_{m1}(t)&=\left[m_1\cos(\omega_1 t)+m_2\cos(\omega_2 t)\right]\\ \phi'_{m1}(t)&=\left[m_1\cos(\omega_1 t+\pi)+m_2\cos(\omega_2 t+\pi)\right]\\ \phi_{m2}(t)&=\left[m_1\cos(\omega_1 t)+m_2\cos(\omega_2 t)\right]\\ \phi'_{m2}(t)&=\left[m_1\cos(\omega_1 t+\pi)+m_2\cos(\omega_2 t+\pi)\right]\end{aligned}\right\} \quad (4)$$

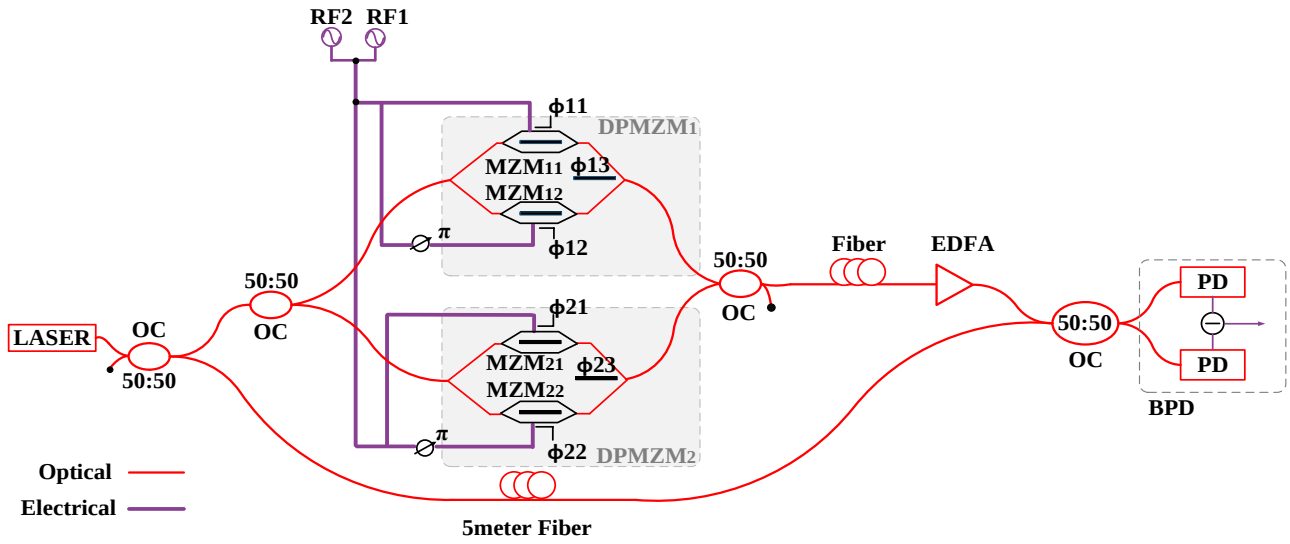

Fig. 1. Schematic diagram of proposed linearization scheme with two input frequencies. BPD: Balanced Photodetector, DPMZM: Dual-Parallel Mach Zehnder Modulator, EDFA: Erbium-doped fiber amplifier, MZM: Mach Zehnder Modulator, OC: Optical Coupler, PD: Photodiode.

In (4), 'm_1' and 'm_2' are the modulation depth for DPMZM1 and DPMZM2, respectively. This is defined as $m_i=\pi V_i/V\pi$ (i = 1, 2), where V_i represents the amplitude of the input i^{th} RF signal. The optical fields of DPMZM1 and DPMZM2 are combined to obtain the transfer function of the D-DPMZM.

$$E_{D-DPMZM}(t) = E_{DPMZM1}(t) + E_{DPMZM2}(t). \tag{5}$$

Assuming $\phi_{ij} = \pi$; (i=1,2; j= 1,2,3), (5) can be further simplified to achieve an optical spectrum with carrier suppression. The suppression of optical carrier in the modulated signal has a great influence on the reduction of power fading and dispersion in the transmission link. Therefore, the overall system performance can be improved. It should be noted that optical carrier is required at the receiver for the recovery of fundamental RF signals. So, an unmodulated optical carrier is transmitted through a separate polarization maintained (PM) fiber and coupled with the modulated signal. The phase change ϕ_{13} and ϕ_{23} are set to π. Hence, (5) can be re-written as below;

$$E_{D-DPMZM} = \frac{E_c}{2} e^{j\omega_c t}\left[\left\{\cos\left(\frac{\phi_{m1}(t)+\pi}{2}\right) - \cos\left(\frac{\phi'_{m1}(t)+\pi}{2}\right)\right\} + \left\{\cos\left(\frac{\phi_{m2}(t)+\pi}{2}\right) - \cos\left(\frac{\phi'_{m2}(t)+\pi}{2}\right)\right\}\right] \tag{6}$$

At the receiver, the optical carrier signal ($E_L(t) = E_L/\sqrt{2}\, e^{j\omega_L t}$) is directly combined with a carrier-suppressed modulated signal by using an optical coupler. A photodiode must have an optical carrier with its sideband signals to retrieve the fundamental frequencies (RF_1 and RF_2) [25]. The two output optical fields from the coupler can be expressed as [26];

$$\begin{bmatrix} E_1(t) \\ E_2(t) \end{bmatrix} = \frac{1}{\sqrt{2}} \begin{bmatrix} E_{D-DPMZM}(t) + jE_L(t) \\ E_L(t) + jE_{D-DPMZM}(t) \end{bmatrix}. \tag{7}$$

The photocurrent $I_{BPD}(t)$ of the balanced photodetector can be determined by substituting output fields of the coupler into the following:

$$I_{BPD}(t) = \Re\left[E_1(t).E_1^*(t) - E_2(t).E_2^*(t)\right] \tag{8}$$

Where, $\Re$ is the responsivity of the photodetector, $E^*_1(t)$ and $E^*_2(t)$ are the conjugates of the actual transfer functions, and both fields are subtracted due to a differential configuration of the BPD. By substituting (4), (6) and (7), to (8), it can be rewritten as;

$$I_{BPD}(t) = 4\Re\frac{E_C}{2}\frac{E_L}{\sqrt{2}}\cos((\omega_C - \omega_L)t)\left\{-4\sin\left(\frac{\phi_{m1}(t)}{2}\right)\right\} \tag{9}$$

The unmodulated carrier frequency is represented as ω_L, and the modulated carrier frequency is denoted as ω_C. Since a single wavelength laser source is used in the proposed system, ω_L and ω_C are equal (same angular frequency). Also, by substituting $\phi_{m1}(t)$ into (9), the photocurrent can be expressed as;

$$I_{BPD}(t) = -\sqrt{2}\Re E_C E_L\left\{\sin\left(\frac{m_1\cos(\omega_1 t) + m_2\cos(\omega_2 t)}{2}\right)\right\} \tag{10}$$

By applying the Jacobi-Anger Expansion in (10), the high order Bessel functions can be expanded to investigate the beating of different frequency components as shown below;

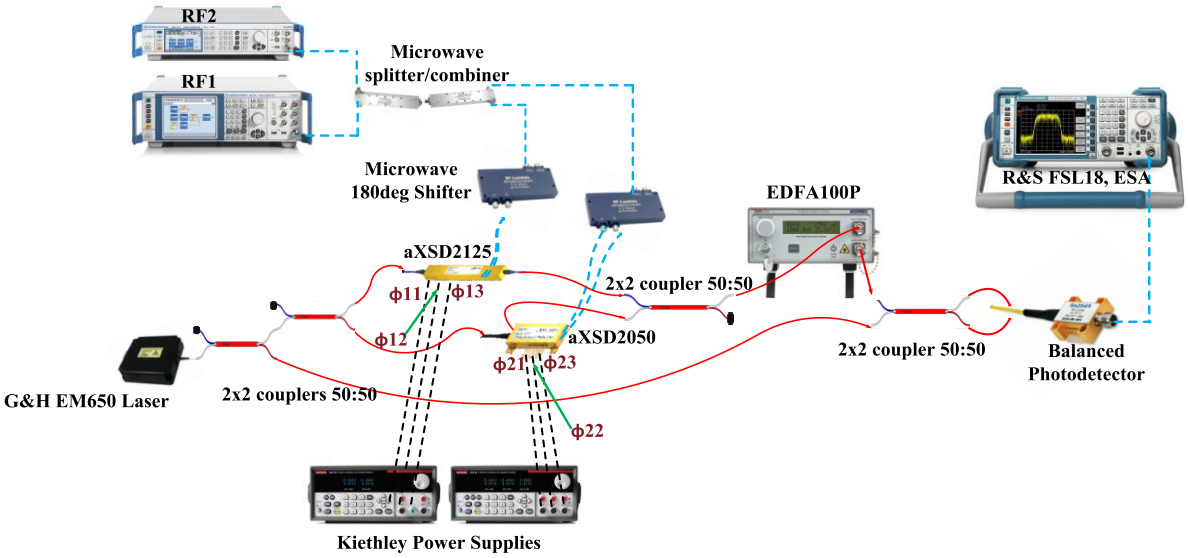

Fig. 2. Experimental setup demonstration of our proposed scheme

$$I_{BPD}(t) = -\sqrt{2}\Re E_C E_L \left\{ \sum_{p,q=-\infty}^{\infty} J_{p,q}\left(\frac{m_i}{2}\right) \sin\left(\begin{matrix} p\omega_1 + q\omega_2 \\ +(p+q)\left(\frac{\pi}{2}\right) \end{matrix} \right) t \right\} \tag{11}$$

By expanding (11), and claiming that p≠q to satisfy the conditions for the elimination of IMD2 and SHD;

$$I_{BPD}(t) = -\sqrt{2}\Re E_C E_L \left[\begin{matrix} J_{0,1}\left(\frac{m_2}{2}\right)\cos(\omega_2 t) \\ +J_{1,0}\left(\frac{m_1}{2}\right)\cos(\omega_1 t) \\ -J_{1,2}\left(\frac{m_1}{2}\right)\left(\frac{m_2}{2}\right)\cos(\omega_1 + 2\omega_2)t \\ -J_{2,1}\left(\frac{m_1}{2}\right)\left(\frac{m_2}{2}\right)\cos(2\omega_1 + \omega_2)t \end{matrix} \right]. \tag{12}$$

In (12), the *jth* order represents the higher order of frequencies. It can be observed that IMD2 and SHD do not exist and are eliminated at the Balanced Photodetector (BPD). However, theoretically, IMD3s still exist and are suppressed immensely, which results in a higher SFDR and Fundamental signal-to-interference ratio (S/I).

III. Experimental Results and Discussions

The proposed APL system configuration illustrated in Fig.1 is now implemented experimentally, as shown in Fig. 2 and Fig.3. In Fig.2, the components used for this experiment are laid out to relate with the schematic diagram from Fig.1. Fig.3 depicts the actual presentation of the experiment in our Microwave Photonics and Sensors (MPS) lab. The experimental setup of the proposed AMPL uses PM fibers and fiber-components, such as Laser source, EDFA, Optical couplers, Modulators**,** and Optical patch cables. The use of PM fibers in the set up contribute**s** to enhancing the system stability in contrast to the use of Single-mode (SM) fibers. A Distributed Feedback Laser source with the following specifications is used; (Gooch & Housego, EM650-193400-100-PM900-FCA-NA), center wavelength 1550nm with an optical output power of 20dBm and Relative Intensity Noise (RIN) of -155dBm/Hz. The RF signals are modulated by two independent GaAs DPMZMs (Axenic, aXMD2050**,** and aXSD2125), which has an RF half-wave voltage of 3V and 4.2V and a bandwidth of up to 50GHz. The two-tone RF signals (RF_1=5GHz and RF_2=5.0005GHz) at an amplitude of 6dBm are generated from the Signal Generators (R&S, SMA100A**,** and SMF100A). It should be stated that the RF signals are combined and split by power dividers (Marki Microwave, PD-0R618), and each electrical input of the DPMZM is phase-shifted to 180°, by using Microwave Hybrid couplers (RF Lambda, RFHB02G18GPI). After processing through these electrical components, the RF signals, become lossy and weak, and the actual incident power of RF signals on the modulator electrodes is measured to be around -2dBm. The optical output of both DPMZMs is coupled by using a 50:50 polarization maintained (PM) optical coupler, where the resultant output is amplified by 20dB with an Erbium-doped fiber amplifier (EDFA) (Thorlabs, EDFA100P). The amplified optical field is finally coupled with an optical carrier from the original laser source. For the experimental demonstration of the proposed architecture, a 5meter PM fiber was used and this length of fiber was chosen based on the estimated optical path length of the modulated transmission link. It was critical to match the path length of modulated and unmodulated transmission link for a common mode rejection ratio. As difference in optical path length can potentially cause discrepancy in optical phases of both paths. This would result in poor cancellation of distortion products at the balanced photodetector. However, in the case of different optical path length an optical delay line can be deployed to correct the phase error. The optical path is approximately matched by measuring the optical fiber lengths used with each component, and a 5-meter PM optical fiber is used to transmit an optical carrier, which is then combined with an amplified

modulated signal by a 50:50 optical coupler. The two optical fields from the coupler are then injected into the inputs of BPD (Finisar, BPDV2120R-VM-FP), where the detector is biased to function as a differential balanced detector. The first and second diodes of the BPD have a responsivity of 0.60A/W and 0.63A/W, respectively. It should be stated that the intrinsic property of BPD also helps in reducing the amplified spontaneous emission (ASE) and relative intensity noise (RIN) from the laser [30]. It is also well known that the increase in laser power by EDFA increases the RIN, which results in the degradation of signal to noise ratio (SNR). However, this degradation in SNR can be avoided by using the differential balanced detector. These benefits of the balanced detector over a single direct photodetector makes it suitable for the proposed scheme [31]. The electrical output of the BPD is analyzed by an electrical spectrum analyzer ESA (R&S, FSL 18). This experiment is developed by using components with polarization maintained (PM) fiber pigtails and connectors, which obsolete the need for any manually or electronically controlled polarization controllers.

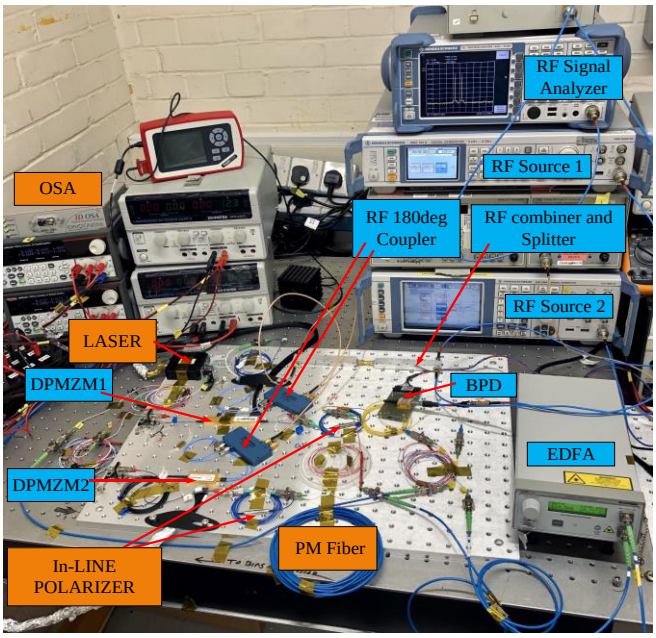

Fig 3. Experimental Setup of the proposed scheme in our Microwave Photonics lab.

Both independent DPMZMs are externally biased by DC supplies to Null the optical carrier, as it is shown in Fig.4. The optical spectrum is observed by using an Optical spectrum Analyzer (ID Photonics OSA). The nulling of the optical carrier is achieved by biasing the sub-MZMs (including a parent sub-MZM) of each DPMZM to a Vπ, and by applying a 180° RF phase shifter to accomplish a phase difference of π between the two input electrical ports of each DPMZM. Fig. 4(a) shows an output of DPMZM1 with the maximum suppression of optical carrier at a level of -63dBm, whereas Fig. 4(b) shows the output spectrum of the DPMZM2, and it depicts the suppression of OC to -66dBm. The difference in the optical power of carrier from both the modulators is 3dB, which is because both devices are not 100% identical, and due to this reason, upon a combination of their output, an increment in the optical carrier peak power can be noticed as shown in Fig. 4(c). The upper sidebands (USB) and lower sidebands (LSB), shown in Fig. 4, are the modulated RF signals, which are the addition and subtraction from the carrier frequency (ω_c). It should be stated that external DC bias sources are used to control the modulators operating point and it is observed that the bias-point of the modulators do not drift over a long period. This validates the properties of the GaAs as mentioned in Walker's article [26]. As it is aforementioned, the suppression of optical carrier helps in limiting the dispersions of an optical signal caused by the nonlinearity of fiber.

Throughout the experiment, it is noticed that the extinction ratio (ER) of each sub-MZM of the DPMZM is not identical, due to this difference in ER, the maximum suppression of optical carrier cannot be achieved. Therefore, we explored the sub-MZM imbalance in the DPMZM by using the VPI simulation model [32], where we found that the maximum suppression in the optical carrier and second-order distortions

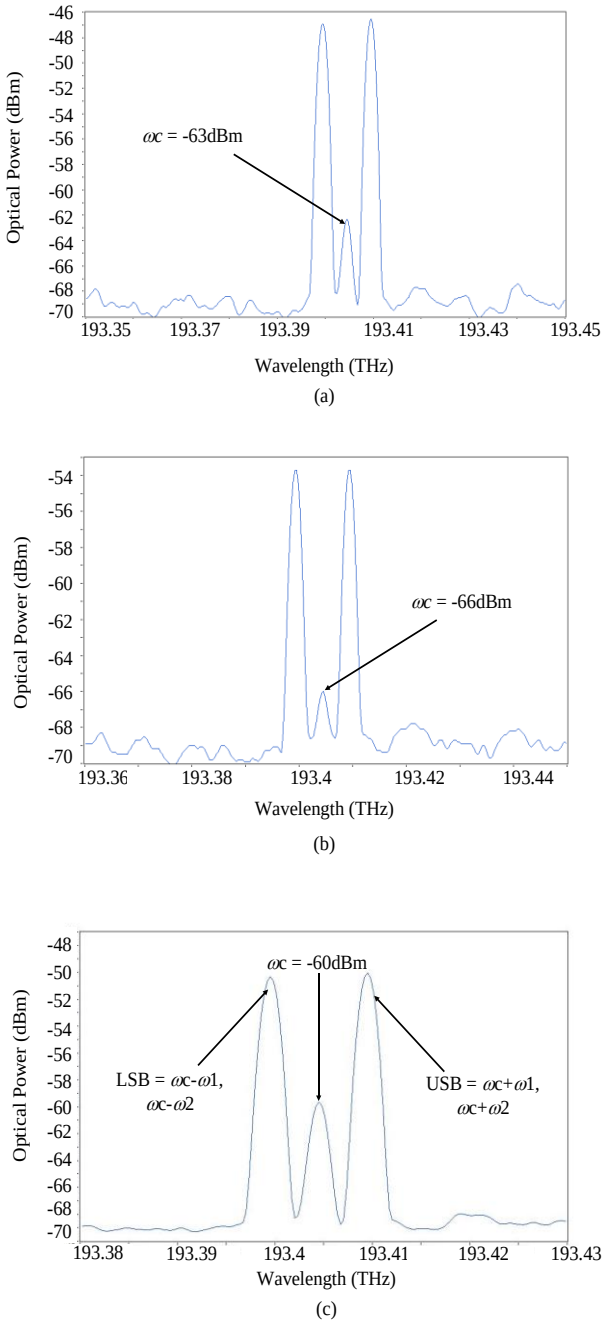

Fig. 4. Measured Optical spectrum of the proposed structure illustrates the highly suppressed carrier (a) Optical spectrum from DPMZM1 (b) Optical Spectrum from DPMZM2 (c) Combined Optical Spectrum of

can only be achieved when the MZM imbalance is zero, as it is shown in Fig. 5. It also illustrates that in a DPMZM, when sub-MZMs are biased to operate at a Null point, the phase relation between the optical carrier and second-order harmonics (SHD) become identical, which is why in Fig. 5, both OC and SHD varies uniformly to each other. In our study, the measured imbalance in the ER of sub-MZMs is 3.3dB, which cannot be externally corrected, and it requires an internal monolithic optical attenuator.

The output of the modulator is amplified by using EDFA, and it is adjusted to limit the incident power on the photodiode to 8dBm. The carrier signal from the laser source

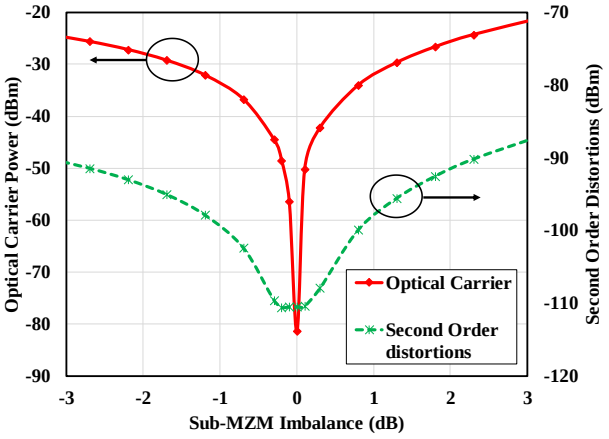

Fig. 5. Sub-MZM imbalance analysis based on a simulation model.

is propagating through 5 meters of PM optical fiber, and it is coupled with the reference modulated signal for the photodetector to retrieve the fundamental RF signals with high efficiency. Both optical fields from the coupler are detected at the BPD, where the differential configuration of the BPD cancels out the even-order distortions (SHD and IMD2). Nevertheless, it should be stated that due to the limitations posed by the components, a complete cancellation of the even-order harmonics is practically impossible. Hence, in Fig. 6(b) IMD2 (10.0005GHz) and SHD (10GHz & 10.001GHz) still exist, but their peak power is around 5dB lower compared to the performances reported in the literature [22].

Concurrently, improvements in the fundamental signal to interference ratio (S/I) are measured and illustrated in Fig. 6(a), which demonstrates that the IMD3s (4.9995GHz & 5.001GHz) are below the noise floor, at a level of -90dBm, with a measured S/I of 60dB.

Fig. 6(c) shows a multi-octave RF spectrum in a range of 4GHz to 11GHz, measured by ESA of a frequency range up to 18GHz. The notch in the spectrum on the surface of the noise floor at around 6GHz is due to an internal band filter of the ESA, which represents a particular band of the spectrum. Even-order distortions are also shown close to the level of the noise floor, which proves that intermodulation distortions are very low. Therefore, it means that a clean multi-octave spectrum can be achieved, and substantially a bandwidth of the AWPL can be maximized.

Another scenario has been tested for the proposed system.

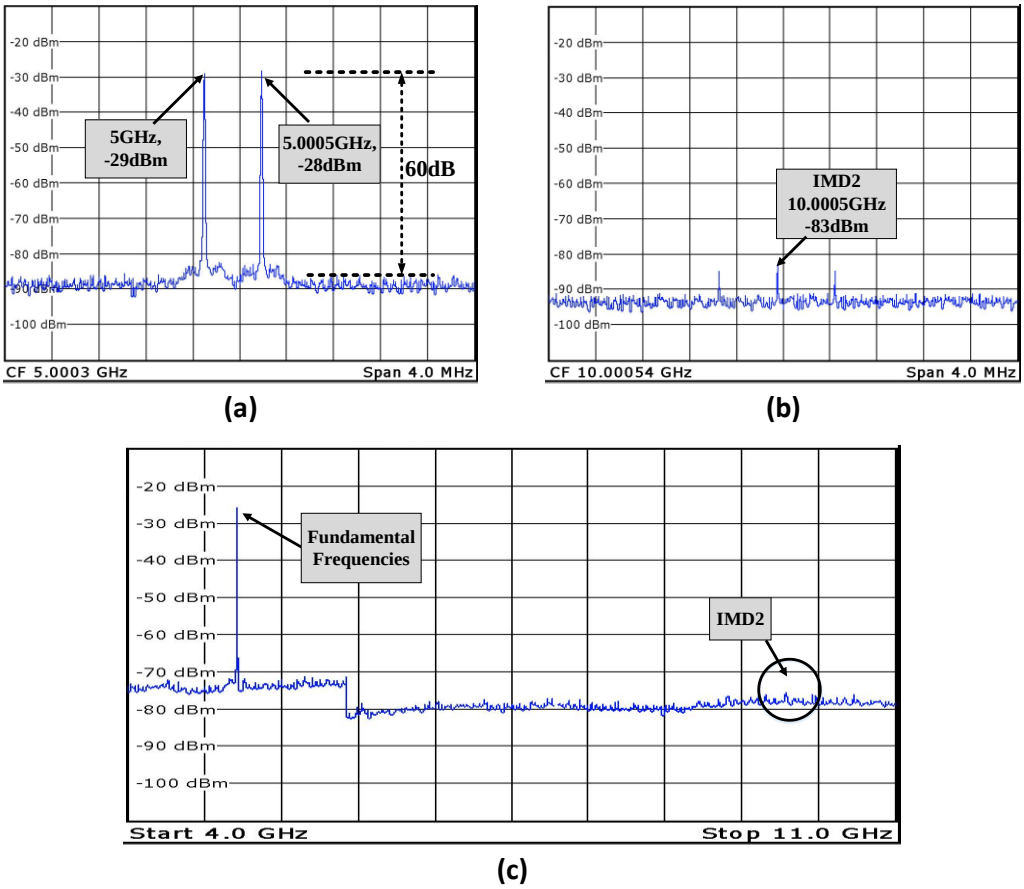

Fig. 6. Measured Electrical Spectrum at the output of BPD (a) Spectrum with Fundamental frequencies and IMD3 (b) Spectrum with Even-Order Distortions (c) Spectrum showing fundamental signals and IMD2s

The second DPMZM in Fig. 1 has similar configuration and the main idea behind the use of second DPMZM is to emulate the architecture of a monolithic polarization multiplexing dual parallel Mach Zehnder modulator (PM-DPMZM). The function of second DPMZM is identical to the first DPMZM, however, it is included to present an additional functionality of second remotely located channel, which is highly favourable in Defence and aerospace applications. In order to further explain this functionality, we have included the experimental results of two channel in Fig. 7. In Fig. 7, the output electrical spectrum has been shown, where four different frequencies are transmitted through two different RF channel. In this case, the first DPMZM was injected with 6.0005GHz and 6GHz, and the second DPMZM was injected with 6.00328GHz and 6.00278GHz. Therefore, it can be stated that the second DPMZM is highly useful for a remotely located channel, where the signals need to be transmitted through a singular optical link.

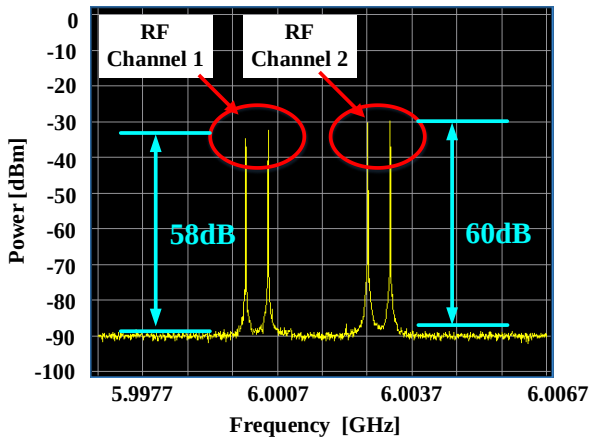

Fig. 7. Output Electrical Spectrum of two Channel

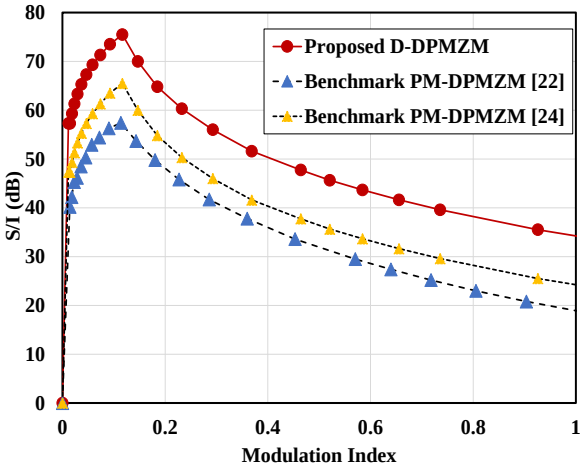

Fig. 8. The Fundamental Signal-to-interference ratio as a function of modulation index

The performance of the proposed AWPL is analyzed at varying modulation index from 0 to 1. The modulation index is a ratio of a drive voltage and a half-wave voltage of the modulator. It is an important performance indicator for every modulation link, which identifies a linear working region of any modulator, where distortions are minimized. In Fig.8, the modulation index is varied, and S/I is measured. It is then compared with the previously reported literature based on PM-DPMZM [22, 24]. It should be stated that the system with a modulation index from 0.05 to 0.2 has a S/I of above 60dB. Beyond this limit, the system performance starts to deteriorate and becomes limited by intermodulation distortions. System with S/I of more than 60dB is considered a linearized system. It is demonstrated that S/I of 75dB can be achieved at a modulation index of 0.12, which is 10dB higher than the PD-DPMZM based method, as shown in Fig. 8. This performance factor indicates that our proposed and developed method is more robust to IMD3s and IMD2s and shows much better performances as compared to any predecessor techniques reported in the literature.

The SFDR performances for IMD3 and IMD2 are analyzed by increasing the input RF power and measuring the changes in the fundamental frequency amplitudes, including measuring the third and second-order intermodulation's amplitude at the output of the BPD. The noise level of the proposed system is

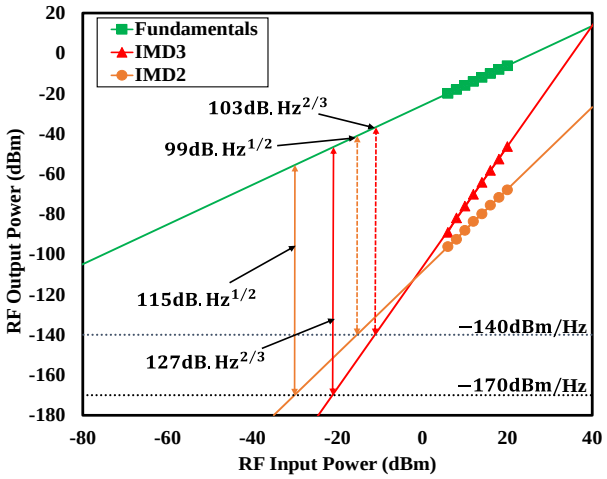

Fig. 9. SFDR performance analysis of IMD3 and IMD2.

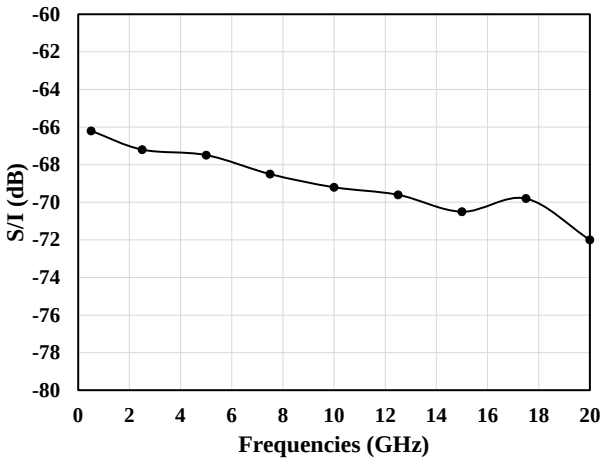

Fig. 10. Performance of the proposed APL at different frequencies

mainly dependent on the shot noise and ASE noise contributions from the EDFA. However, the BPD reduces the RIN noise and ASE noise, which substantially decreases the noise floor to -170dBm/Hz. The noise floor was estimated to be at -170dBm/Hz. However, the measured noise floor from the electrical spectrum analyzer is -140dBm/Hz. Thus, the SFDR2 and SFDR3 with respect to the measured noise floor is 99dB.$Hz^{1/2}$ and 103dB.$Hz^{2/3}$, respectively. This has been

shown in Fig 9. The path length of both the optical inputs of BPD is kept similar so that noise levels can be reduced, and SFDR performance can be enhanced [32]. The reported values of SFDR2 and SFDR3 in [24] are 95.5dB.Hz$^{1/2}$ and 123.9dB.Hz$^{2/3}$. From Fig. 9, it can be seen that the IMD2 and IMD3 are increased by 19.5dB and 3.1dB, respectively.

The performance of the proposed system is further analyzed at different frequency ranges. In Fig. 10, the signal-to-interference ratio (S/I) has been investigated at a frequency range of 0.5GHz to 20GHz. It is observed from the results that the performance of the system deteriorates at higher frequencies.

IV. Conclusion

In this paper, we proposed, and theoretically & experimentally demonstrated an improved linearized multi-octave AMPL system with eliminated even-order distortions from the RF spectrum at the output of the detector/receiver. The mathematical model has been developed and fully validated against the experimental. The RF phase and DC bias of the modulator has been optimized to achieve the maximum possible suppression in the optical carrier. The carrier suppressed double-sideband signals have been transmitted over the proposed AMPL to limit the introduction of additional dispersions from the optical fiber. It has been proved that even order harmonics can be eliminated by using the proposed method and the overall improvement in SFDR2 and SFDR3 of 115dB.Hz$^{1/2}$ and 127dB.Hz$^{2/3}$ has been achieved, respectively. To the best of our knowledge, we have reported the highest performance of AMPL system, using a GaAs electro-optic (EO) modulator. These modulators overcome the issue of bias drift due to environmental effects on the device. Therefore, it can be stated that the system is robust and suitable for operating in a harsh environment. It can also be noted that the system provides a high signal to interference ratio regardless of the system limitations such as the ASE noise induced by the EDFA amplification. However, ASE filter can be used to further reduce the EDFA noise. The biasing of the two dual-parallel Mach-Zehnder modulator needs to be precisely controlled, which can be improved in future by using an automated bias controller. The fundamental signal to interference ratio (S/I) can also be further enhanced by using polarization combiners to overcome the losses from the optical combiners.

References

[1] J. Yao, "Microwave Photonics," in *Journal of Lightwave Technology*, vol. 27, no. 3, pp. 314-335, Feb.1, 2009.

[2] R. W. Ridgway, C. L. Dohrman and J. A. Conway, "Microwave Photonics Programs at DARPA," in *Journal of Lightwave Technology*, vol. 32, no. 20, pp. 3428-3439, Oct.15, 2014.

[3] J. Capmany and D. Novak, "Microwave photonics combines two worlds," Nat. Photonics, vol. 1, no. 6, pp. 319-330, June 2007.

[4] F. Paloi, S. Haxha, T. Mirza, M. Alom, "Microwave Photonic Downconversion With Improved Conversion Efficiency and SFDR. *IEEE Access*. 6, p. 8089-8097, Jan. 2018.

[5] T. Mirza, S. Haxha, and I. Flint, "Reduction of Intermodulation Distortions and Even Order Harmonics of two or more microwave signals" Patent Application Number: GB1900552.9, Filing date: 15 January 2019.

[6] I. Flint, S. Haxha, and T. Mirza, "A method of driving an MZM, mixer and SSBs post manufacture to trim out intensity errors", Patent Application Number: GB1821175.5. Filing date: 24 December 2018.

[7] S. Shaqiri, S. Haxha, and T. N. Mirza, "Elimination of odd and even intermodulation distortions of analog microwave photonics link based on GaAs MZMs," in Opt. Express, vol. 28, pp. 17521-17531, June 2020.

[8] B. M. Haas and T. E. Murphy, "A Simple, Linearized, Phase-Modulated Analog Optical Transmission System," in *IEEE Photonics Technology Letters*, vol. 19, no. 10, pp. 729-731, May15, 2007.

[9] W. B. Bridges and J. H. Schaffner, "Distortion in linearized electrooptic modulators," in *IEEE Transactions on Microwave Theory and Techniques*, vol. 43, no. 9, pp. 2184-2197, Sept. 1995.

[10] S. Granieri and A. Siahmakoun, "Optical modulation with a single sideband and carrier suppressed," Proc. SPIE, vol. 4883, pp. 1154–1158, 2002.

[11] X. J. Meng and A. Karim, "Microwave photonic link with carrier suppression for increased dynamic range," Fiber Integr. Opt., vol. 25, no. 3, pp. 161–174, 2006.

[12] M. L. Farwell, W. S. C. Chang, and D. R. Huber, "Increased linear dynamic range by low biasing the Mach-Zehnder modulator," *IEEE Photon. Tech. Lett., vol.* 5(7), pp. 779–782, July 1993.

[13] M. J. Lagasse, W. Charczenko, M. C. Hamilton, and S. Thaniyavarn, "Optical carrier filtering for high dynamic range fiber optic links," *Electron. Lett*., vol. 30, pp.2157–2158, Dec 1994.

[14] Z. Chen, L.Yan, W. Pan, B. Luo, X. Zou, Y. Guo, H.Jiang and T.Zhou, "SFDR enhancement in analog photonic links by simultaneous compensation for dispersion and nonlinearity," Opt. Express, vol. 21, no. 18, pp. 20999–21009, 2013.

[15] S.Wang, Y.Gao, A.Wen and L, Liu, "A microwave photonic link with high spurious-free dynamic range based on a parallel structure," Optoelectron. Lett., Vol. 11, no. 2, pp. 137-140, 2015.

[16] X. Li, Z. Zhu, S. Zhao, Y. Li, L. Han, and J. Zhao, "An intensity modulation and coherent balanced detection intersatellite microwave photonic link using polarization direction control," Optics & Laser Technology, vol. 56, pp. 362-366, 2014.

[17] Y. Cui, Y. Dai, F. Yin, J. Dai, K. Xu, J. Li, and J. Lin, "Intermodulation distortion suppression for intensity-modulated analog fiber-optic link incorporating optical carrier band processing," Opt. Express, vol. 21, no. 20, pp. 23433-23440, 2013.

[18] A. Karim and J. Devenport, "Low Noise Figure Microwave Photonic Link," *2007 IEEE/MTT-S International Microwave Symposium*, Honolulu, HI, pp. 1519-1522, 2007.

[19] J. Li, Y. Zhang, S. Yu, T. Jiang, Q. Xie, and W. Gu, "Third-order intermodulation distortion elimination of microwave photonics link based on integrated dual-drive dual-parallel Mach–Zehnder modulator," Opt. Lett., vol. 38, no. 21, pp. 4285-4287, 2013.

[20] W. Jiang, Q. Tan, W. Qin, D. Liang, X. Li, H. Ma, and Z. Zhu, "A Linearization Analog Photonic Link With High Third-Order Intermodulation Distortion Suppression Based on Dual-Parallel Mach–Zehnder Modulator," in *IEEE Photonics Journal*, vol. 7, no. 3, pp. 1-8, 2015.

[21] Y. Cui, Y. Dai, K. Xu, F. Yin and J. Lin, "Multi-octave operation of analog optical link using parallel intensity modulators," *Optical Communications and Networks (ICOCN), 2013 12th International Conference on*, Chengdu, pp. 1-4, 2013.

[22] D. Zhu, J. Chen, and S. Pan, "Multi-octave linearized analog photonic link based on a polarization-multiplexing dual-parallel Mach-Zehnder modulator," Opt. Express, vol. 24, no. 10, pp. 11009-11016, 2016.

[23] Y. Wang et al., "Microwave Photonic Link with Flexible Even-Order and Third-Order Distortion Suppression," in IEEE Journal of Quantum Electronics, vol. 55, no. 3, pp. 1-9, June 2019.

[24] Q. Tan, Y. Gao, Y. Fan, and Y. He, "Multi-octave analog photonics link with improved second- and third-order SFDRs," *Optics Communications*, vol. 410, pp. 685-689, 2018.

[25] X. Han, X. Chen, and J. Yao. "Simultaneous even- and third-order distortion suppression in a microwave photonic link based on orthogonal polarization modulation, balanced detection and optical sideband filtering," Optics Express, vol. 24, no. 13, pp. 14812-14827, June 2016.

[26] R.G. Walker, N. Cameron, Y. Zhou, and S. Clements, "Electro-Optic modulators for space using Gallium Arsenide," Proc. SPIE 10562, International Conference on Space Optics-ICSO 2016, 105621A, September 2017.

[27] R.G. Walker, I Bennion and A C Carter; "Low voltage, 50Ω GaAs/AlGaAs travelling-wave electro-optic modulator with bandwidth exceeding 25GHz", Electron. Lett., 25(23), pp. 1549–1550,1989.

[28] G. Zhu, W. Liu and H. R. Fetterman, "A Broadband Linearized Coherent Analog Fiber-Optic Link Employing Dual Parallel Mach–Zehnder Modulators," in *IEEE Photonics Technology Letters*, vol. 21, no. 21, pp. 1627-1629, 2009

[29] W. Qin and W. Jiang, "The performance analysis of microwave photonic frequency conversion using double-sideband suppressed-

carrier and balance detection," in *IEEE International Conference on Communication Problem-Solving (ICCP)*, pp. 582-585, Guilin, 2015.
[30] C. Middleton and R. DeSalvo, "High performance microwave photonic links using double sideband suppressed carrier modulation and balanced coherent heterodyne detection," *MILCOM 2009 - 2009 IEEE Military Communications Conference*, Boston, MA, , pp. 1-6, 2009.
[31] J. Kim, W. B. Johnson, S. Kanakaraju, W. N. Herman, C. H. Lee, "Demonstration of balanced coherent detection using polymer optical waveguide integrated distributed traveling-wave photodetectors", *Opt. Express*, vol. 17, no. 22, pp. 20242-20248, 2009
[32] D. Marpaung, C. Roeloffzen, A. Leinse, and M. Hoekman, "A photonic chip based frequency discriminator for a high performance microwave photonic link," *Opt. Express*, vol. 18, pp. 27359-27370, 2010.

Dr. TAIMUR NAZIR MIRZA Received his BEng (Hons) in Electrical and Electronics Engineering in 2013 and MSc in Embedded Intelligent Systems in 2014 from the University of Hertfordshire in United Kingdom. Later in 2020, he was awarded a PhD in Electronics Engineering from Royal Holloway University of London. Currently He is working as a Research Assistant at the Royal Holloway University of London. His research interests include the Optical signal processing and filtering, and long-haul transmission in the Radio-over fiber system.

Dr. SHYQYRI HAXHA (SM'14) received the MSc and PhD degrees from City University in London in 2000 and 2004, respectively. He has also obtained several world-class industrial trainings and diplomas such as Executive MBA Cambridge Judge Business School and Mini Telecom MBAs. He was awarded the SIM Postgraduate Award from The Worshipful Company of Scientific Instrument Makers in Cambridge for his highly successful contribution in research. Currently, he is a Reader at Royal Holloway, University of London, Department of Electronic Engineering Egham, Surrey, United Kingdom. He was also a Reader in Photonics in the Computer Science and Technology, University of Bedfordshire, Luton in the United Kingdom. Prior to these posts, he was a lecturer in Optic Communication at the School of Engineering and Digital Arts, University of Kent, Canterbury, United Kingdom.
Dr Haxha expertise is focused on designing and optimizing, photonic and microwave devices, and systems for applications in Sensor Technology (Medical and Environmental), Nanotechnology and Telecommunication Systems. Dr Haxha research interests are in the areas of microwave photonics, photonic crystal devices, metamaterials, photonic crystal fibres, nano-sensors, optical sensors, surface plasmon polaritons (SPP), biosensors, ultra-high-speed electro-optic modulators, compact integrated optic devices, Optical CDMA, Optical FDM, and Optical MIMO systems. He has developed and demonstrated RF over fibre transmission systems for the aviation industry, including cybersecurity protection for commercial and defense applications.
Dr. Haxha has extensive expertise in Telecommunication Management Industry. He was a Telecommunication CEO in partnership with Cable & Wireless Communications Ltd., a British multinational telecommunications company, and Monaco Telecom International. He is a Chartered Engineer (CEng), Senior Member of the Institution of Electrical and Electronics Engineers (Senior MIEEE), Fellow of the Higher Education Academy (FHEA), Editorial Board Member for MDPI journals and Associate Editor of IEEE Sensors Journal. He has been a keynote speaker of numerous world class conferences.

Prof. IYAD DAYOUB is professor of Communications Engineering; He has been awarded BEng (Telecommunications & Electronics) in 1993. He received the M.A.Sc degree in Electrical Engineering from the National Polytechnic Institute of Lorraine (INPL), and a PhD in 2001 from Valenciennes University/Institute of Electronics, Microelectron-ics and Nanotechnology (IEMN),. He has worked as a system Engineer with Siemens and as a Researcher with Alcatel Business Systems Alcatel, Colombes (Paris). His current research activities at the IEMN of Université Polytechnique Hauts de France (UPHF) are focused on Wireless Communications, 5G technologies & Beyond, Intelligent Transportation Communications, and Radio over Fiber communications. He was (2007-2014) member of the National Council of Universities (CNU, France) in the area of Electrical engineering, electronics, photonics and systems, and Adjunct Professor in Concordia University, Montreal (2010-2014). He is IEEE Senior member, and member of several International Conference Advisory Committees, Technical Program Committees and Organization Committees such as VTC, GLOBECOM, ICC, PIMRC, WWC, etc.